Pattern Recognition Letters 31 (2010) 1388–1395

Contents lists available at ScienceDirect

Pattern Recognition Letters

journal homepage: www.elsevier.com/locate/patrec

An approach based on self-organizing map and fuzzy membership for decomposition of mixed pixels in hyperspectral imagery

Lifan Liu [a], Bin Wang [a,b,*], Liming Zhang [a]

[a] Department of Electronic Engineering, Fudan University, Shanghai 200433, China
[b] The Key Laboratory of Wave Scattering and Remote Sensing Information, Ministry of Education, Fudan University, Shanghai 200433, China

ARTICLE INFO

Article history:
Received 1 March 2009
Received in revised form 27 December 2009
Available online 31 March 2010
Communicated by T. Vasilakos

Keywords:
Mixed pixel
Spectral unmixing
Endmember
Abundance
Self-organizing map neural network
Fuzzy membership

ABSTRACT

Spectral unmixing, which decomposes the mixed pixel into typical ground signatures (endmembers) and their fractional proportions (abundances) is a meaningful job for high-accuracy ground object recognition and quantitative remote sensing analysis. In this paper, a method for decomposition of mixed pixels which combines competitive neural network and fuzzy clustering, termed self-organizing map and fuzzy membership (SOM&FM) is proposed. The proposed method only demands some data samples as prior knowledge to train the SOM neural network in a supervised way. And the unmixing is based on the fuzzy model, which satisfies the abundances non-negative constraint (ANC) and the abundances summed-to-one constraint (ASC) automatically. Experimental results on synthetic and real hyperspectral data demonstrate that the proposed method can be used for both linear and nonlinear spectral mixture situations, and has good unmixing performances.

1. Introduction

The limited spatial resolution of remote sensing images (*e.g.*, the spatial resolution of the AVIRIS hyperspectral remote sensing images is 17×17 m) brings the wide existence of mixed pixels. By decomposing mixed pixels to typical ground objects (endmembers) in fractional proportions (abundances), we can acquire information in sub-pixel level to improve the accuracy of ground object classification and recognition, and to realize the quantitative analysis of remote sensing images (Chang, 2007).

The mixing can be modeled as a linear or nonlinear process depending on endmember distribution (Jia and Qian, 2007). Linear Spectrum Mixture Model (LSMM) (Small, 2001) is available when different endmembers do not interfere with each other, and influential LSMM-based algorithms include Fully Constrained Least Squares (FCLS) (Heinz and Chang, 2001), Gradient Descent Maximum Entropy (GDME) (Miao et al., 2007), Independent Component Analysis (ICA) (Wang and Chang, 2006; Mohamed et al., 2004), and Non-negative Matrix Factorization (NMF) (Miao and Qi, 2007; Paura et al., 2006), *etc*. The ICA method is proved to be useful for the mixed pixel decomposition only when the number of endmembers is large enough, because a small number of endmembers means the strong correlation between endmembers due to the abundances summed-to-one constraint (ASC), which contradicts with the independent assumption in the ICA. The NMF method decomposes a mixed matrix into a source matrix and a mixing matrix, which are both non-negative. Consequently, the abundances non-negative constraint (ANC) is satisfied automatically. However, main problem of the NMF method should focus on how to avoid dropping into the local optimum. On the other hand, when multiple scattering between different endmembers cannot be ignored (commonly referred to as the *intimate mixture*), the measured spectrum is no longer a linear combination of the constituent spectrum. For example, when describing the mixtures of soil and vegetative surfaces, Nonlinear Spectrum Mixture Model (NSMM) is more appropriate to describe this mixing process (Jia and Qian, 2007).

In this letter, we present a new unmixing method which combines self-organizing map neural network and fuzzy membership (SOM&FM) for mixed pixel decomposition in remote sensing images, and we use experiments to demonstrate that it is suitable for decomposition of mixed pixels, especially for nonlinear spectral mixing. This new method includes three parts: the training of SOM neural network, the calculation of fuzzy membership, and the abundance estimation. It satisfies the ANC and ASC conditions automatically and has not the risk of falling into local minimum.

The remainder of this paper is organized as follows. Sections 2 and 3 introduce the supervised SOM neural network and the definition of fuzzy membership, respectively. Section 4 describes the

* Corresponding author at: The Key Laboratory of Wave Scattering and Remote Sensing Information, Ministry of Education, Fudan University, Shanghai 200433, China.

E-mail addresses: 062021032@fudan.edu.cn (L. Liu), wangbin@fudan.edu.cn (B. Wang), lmzhang@fudan.edu.cn (L. Zhang).

0167-8655/$ - see front matter © 2010 Elsevier B.V. All rights reserved.
doi:10.1016/j.patrec.2010.03.020

proposed method for decomposition of mixed pixels. Experimental results are shown in Section 5 and conclusion is in Section 6.

2. The supervised SOM neural network

The traditional SOM neural network is unsupervised (Kohonen, 2001). For abundance estimation, a tagging technique is applied on the training samples to realize the supervised version of SOM, shown in Fig. 1.

Suppose the original dimension of training samples is N, and the number of endmembers is k (*e.g.*, $k = 3$ in Fig. 1). By expanding the dimension of training samples to $N + k$, the class information is embedded into the training samples in the form of binary coding.

Using these training samples with class information to train the SOM neural network, the dimension of the nodes in the competitive layer after training is also $N + k$. For each node, if the value of the ith dimension is the maximum of the front k dimensions, the node can be judged to belong to the ith endmember. After the class information is obtained, the first k dimensions of nodes can be removed. Fig. 2 shows the SOM neural network after supervised training. The nodes in competitive layer with the same color have the same class tag. In another word, they belong to the same endmember.

The reason why we introduce the SOM neural network is that: the endmembers are usually unknown in many unmixing applications. And many endmember estimation algorithms cannot get rid of the problem of local optimum, such as Fuzzy C-Means which would be described in the following section. With the use of SOM neural network training, we could learn the distribution of data samples which would be stored in the SOM nodes. Unmixing based on these SOM nodes is proved to be accurate and effective by experiments of Section 5. And the SOM training is a kind of supervised training without any problem of local optimum.

3. The fuzzy membership

3.1. The fuzzy C-means algorithm

In this subsection, the Fuzzy C-Means (FCM) algorithm (Friedman and Kande, 1999; Foody, 2000) which can be used for decomposition of mixed pixels is introduced. But as the following description shows, the FCM algorithm suffers from slow convergence speed and easily drops into local optimum if it is applied directly for decomposition of mixed pixels. The similarity between the FCM algorithm and the proposed algorithm is that they are both based on fuzzy model, but the difference is that in the proposed algorithm, we only make use of fuzzy membership to represent abundance, instead of using the FCM algorithm to estimate

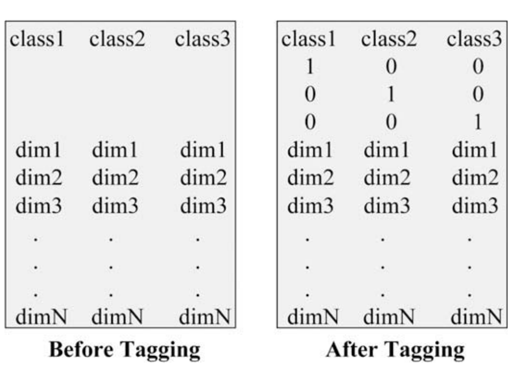

Fig. 1. The tagging technique for training samples.

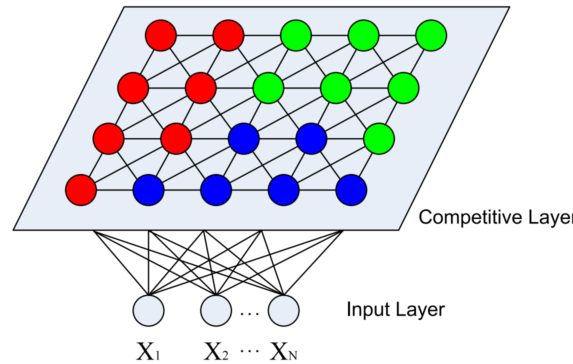

Fig. 2. The SOM neural network after supervised training.

the endmembers, we will use SOM neural network to get the distribution of the data samples which surround endmembers.

As an improvement of the Hard C-Means (HCM) algorithm, the FCM algorithm divides all data samples x_i ($i = 1, 2, \ldots, n$) into c fuzzy classes, and gets the c clustering centers by minimizing the objective function of non-similarity. Instead of using hard classification in the HCM algorithm, the FCM algorithm uses fuzzy classification to represent the similarity between data sample and clustering center by a value (known as *fuzzy membership*) among [0, 1]. And the fuzzy memberships satisfy a constraint formulated as follows:

$$\sum_{i=1}^{c} u_{ij} = 1, \quad \forall j = 1, \ldots, n, \tag{1}$$

where u_{ij} is the membership of the jth data sample to the ith class.

The solution of the FCM algorithm can be obtained by minimizing the objective function as follows:

$$\begin{aligned}\bar{J}_m(U, c_1, \ldots, c_c,\ \lambda_1, \ldots, \lambda_n) &= J_m(U, c_1, \ldots, c_c) + \sum_{j=1}^{n} \lambda_j \Big(\sum_{i=1}^{c} u_{ij} - 1\Big) \\ &= \sum_{i=1}^{c} \sum_{j}^{n} u_{ij}^m d_{ij}^2 + \sum_{j=1}^{n} \lambda_j \Big(\sum_{i=1}^{c} u_{ij} - 1\Big),\end{aligned} \tag{2}$$

where $d_{ij} = \|c_i - x_j\|$ and is the Euclidean distance between the ith clustering center and the jth data sample, $m \in [1,\infty)$ and is a fuzzy weighted index, and λ_j ($j = 1, 2, \ldots, n$) is the jth Lagrange coefficient of the objective function.

By making the derivatives of all λ_j ($j = 1, 2, \ldots, n$) to be zero, the iterative steps of the FCM algorithm can be described as follows:

Step 1: Initiate the clustering centers in random way.
Step 2: Calculate the fuzzy memberships as follows:

$$u_{ij} = \frac{1}{\sum_{k=1}^{c} \left(\frac{d_{ij}}{d_{kj}}\right)^{2/(m-1)}}. \tag{3}$$

Step 3: Calculate the new clustering centers as follows:

$$c_i = \frac{\sum_{j=1}^{n} u_{ij}^m x_j}{\sum_{j=1}^{n} u_{ij}^m}. \tag{4}$$

Step 4: Judge whether the algorithm converges or not by the differences between the clustering centers of last time and current time. Then stop iteration if converging, else jump to Step 2.

Because the clustering centers correspond to the endmembers and the fuzzy memberships correspond to the abundances, the FCM algorithm can be used directly for decomposition of mixed pixels, and the ANC and ASC could be satisfied automatically due to the value location of the fuzzy membership and the Eq. (1). But as the above iterative steps of the FCM algorithm show, all data samples need to be traversed at each iteration. As a result, when the total number of data samples is large, the computational burden becomes heavy. Then the converging speed is slow, and also the algorithm has the risk of falling into the local minimum.

As Section 4 shows, instead of using the FCM algorithm directly, the proposed method only takes use of the concept of fuzzy membership formulated as shown in (3).

3.2. The choice of fuzzy weighted index

In the formulation of fuzzy membership shown as (3), the fuzzy weighted index m determines the fuzzy degree of the unmixing result. The larger the m is, the fuzzier the unmixing result is. When $m = 1$, the unmixing result retrogresses to the hard classifying result. On the other hand, when $m \to \infty$, the unmixing result is over fuzzy, which result in that the memberships of every data sample to each fuzzy class are all equal to $1/c$.

How to choose the fuzzy weighted index m is a problem which puzzles the researchers in the fuzzy theory area for a long time. Some experiential ranges of m for different applications have been proposed by researchers (Yu et al., 2004). Here, a fuzzy weighted index choosing method is introduced, which is based on the inflexion of the fuzzy objective function (Gao et al., 2000) defined as follows:

$$U_g = \exp\left\{-a\frac{J_m(U,c)}{\max_{\forall m}(J_m(U,c))}\right\}, \tag{5}$$

where $J_m(U,c)$ is same to $J_m(U,c_1,\ldots,c_c)$ in (3), and a is a constant which is larger than 1. Fig. 3 shows the curve of the fuzzy objective function, and the fuzzy weighted index m is chosen corresponding to the inflexion of this curve. The effectiveness of this choosing method will be validated in the following experiments.

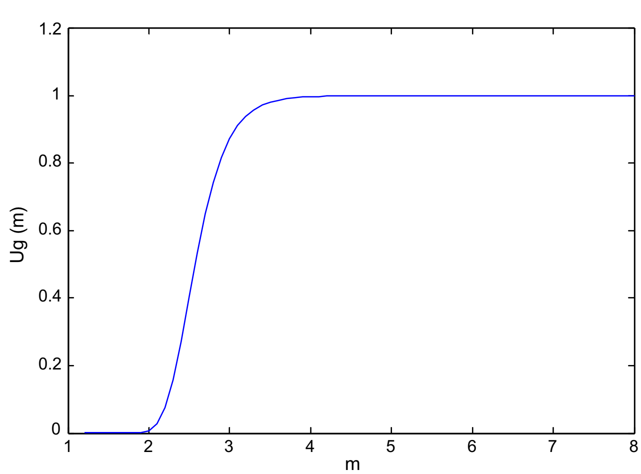

Fig. 3. The curve of the fuzzy objective function.

4. Abundance estimation

Fig. 4 shows the framework of the proposed algorithm for abundance estimation. The details of the proposed algorithm can be described as follows:

Step 1: *Initiation*
(a) Set the parameters of SOM neural network, including the size of the competitive layer, the topological structure, the initial learning rate, and the initial neighborhood radius.
(b) Initiate the competitive layer in random way.
(c) Obtain the training samples as input for training the SOM neural network in next step.

Step 2: *Training*
The training process of the SOM neural network is a kind of competitive learning without any objective function, and thus, any problem of local optimum does not exist there.
(a) Embed class tag into training samples by the tagging technique described in Section 2.2.
(b) With these training samples as input, train the SOM neural network until it converges.
(c) Get the class information of each node in the competitive layer from its expanded tag dimensions, and then remove these dimensions to recover the original dimension.

Step 3: *Membership calculation*
For every mixed pixel, calculate its fuzzy membership to each node in the competitive layer of the SOM neural network after training.

Step 4: *Abundance calculation*
In Step 2, the class information of each node in the competitive layer has been obtained. In Step 3, the fuzzy membership of the mixed pixel to each node has been calculated. In this step, the fuzzy memberships with the same class information are summed together. And the summation is the estimated abundance corresponding to the specified endmember.

In conclusion, we combined the fuzzy model and the SOM neural network and proposed a new unmixing method for mixed pixels in remote sensing images. In the following section, we prove its validity, and its advantages compared to existing methods, and use it in some real application.

5. Experimental results

5.1. Experiments for synthetic images

For the synthetic remote sensing images, the standard abundances are known, so we can evaluate algorithm by root mean square error (RMSE) and correlation coefficient (CC) (an average value is given in the following experiments) between the unmixing

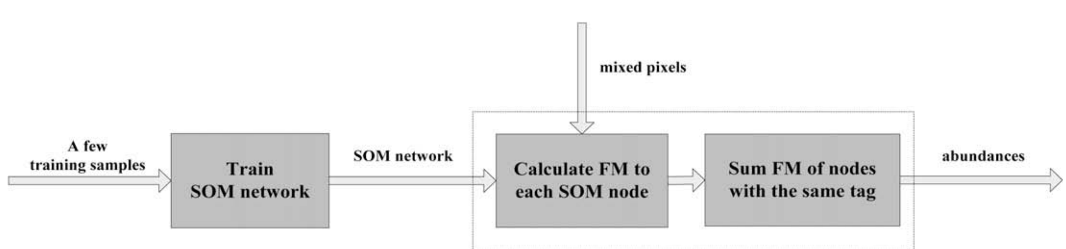

Fig. 4. The framework of the proposed algorithm.

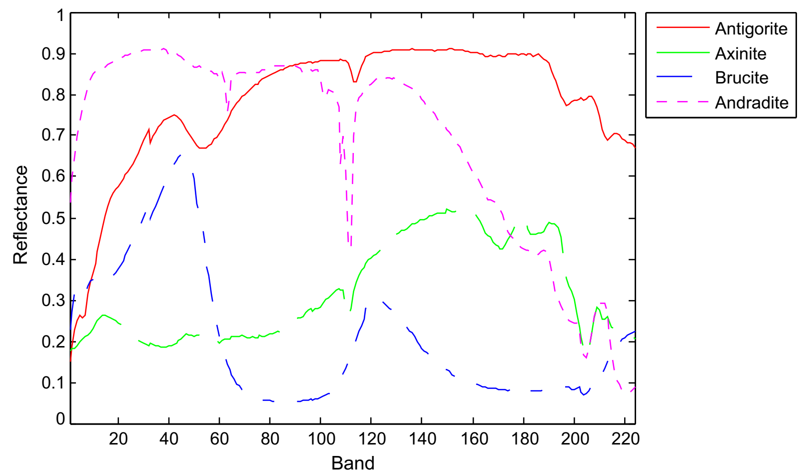

Fig. 5. The four endmembers chosen from AVIRIS Cuprite Spectral Lib.

abundance fractions and standard abundance fractions. We wish the RMSE to be small and the CC to be large as possible.

5.1.1. Simulated hyperspectral images

In this subsection, the experiment is designed to evaluate the influence of the fuzzy weighted index and the network size.

The synthetic image is generated by linear mixing of four mineral endmembers which their spectral signatures are shown in Fig. 5. The four endmembers with 220 bands are chosen from Airborne Visible/Infrared Imaging Spectrometer (AVIRIS) Cuprite Endmember Spectral Lib. The corresponding simulated abundance images which satisfy both the ANC and the ASC shown in Fig. 6. The abundance fractions are larger in the brighter areas.

5.1.1.1. The influence of fuzzy weighted index. Fig. 7 shows the influence of the fuzzy weighted index m to the unmixing result. The broken line is the 1-order derivative curve of fuzzy objective function, and the real line is the RMSE curve of unmixing results under different choices of m. As Fig. 7 shows, the inflexion of fuzzy objective function (in another word, the maximum of its 1-order derivative) points to the minimum of RMSE curve accurately. This also validates the effectiveness of the choosing method of the fuzzy weighted index described in Section 3.2.

5.1.1.2. The influence of network size. In the proposed method, the size of the SOM competitive layer has some influence on the unmixing result. Table 1 shows the unmixing results under different sizes.

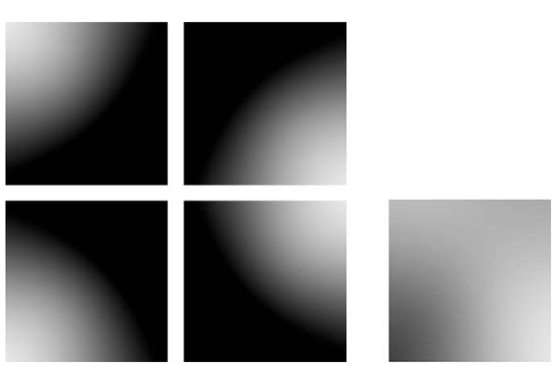

Fig. 6. Standard abundance images (left) and the 150th AVIRIS Cuprite Spectral Lib band of synthetic images (right) (size: 100×100).

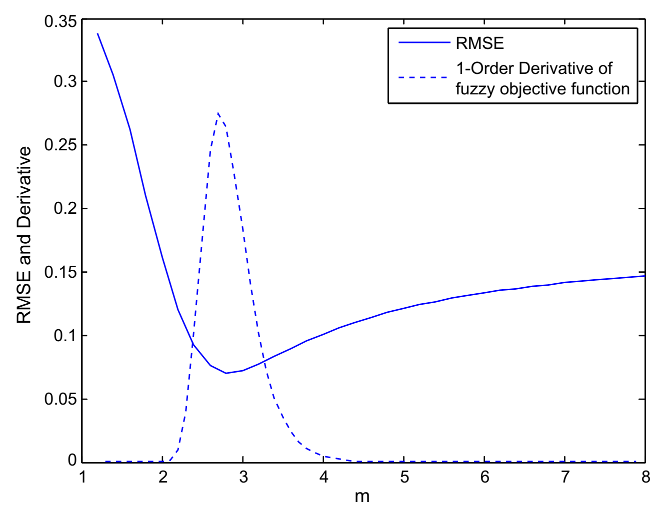

Fig. 7. The choice of m in the experiment of simulated hyperspectral data.

Table 1
The influence of network size.

Size	4×4	8×8	10×10	12×12	15×15	18×18	20×20
CC	0.9351	0.9454	0.9511	0.9563	0.9558	0.9524	0.9549
RMSE	0.1045	0.0811	0.0769	0.0736	0.0761	0.0775	0.0751

As Table 1 shows, the unmixing accuracy advances with the increase of the network size. But after the size has been expanded to 12×12, the unmixing accuracy tends to saturation, which means a larger size will not bring much accuracy improvement any more, but will bring about more training time.

5.1.2. Monte Carlo simulations

In this subsection, we design simulated experiments to evaluate the unmixing accuracy and justify the advantages of the proposed method compared to existing methods. We choose FCM, FCLS and GDME for comparison, because firstly FCM uses the same fuzzy model as our method, but without SOM neural network, so we could see the performance improvement with introduction of SOM learning. Secondly, both FCM and the proposed method are based on nonlinear fuzzy unmixing model. To make the comparison more complete, we give the results of two state-of-art linear unmixing methods: FCLS and GDME, to compare the performance differences between nonlinear fuzzy unmixing model and linear unmixing model in different cases. The synthetic images are created by linear or nonlinear spectral mixture of three AVIRIS Cuprite endmembers and constrained abundances which are generated in a random way. The synthetic images will be decomposed by FCLS, GDME, FCM, and SOM&FM, respectively, and the unmixing abundances will be compared with the standard abundances to evaluate the unmixing accuracy. Two kinds of endmember sets are tested as Fig. 8 shows. One set has significantly distinct endmembers, and another set has endmembers similar to each other. In addition, 100 Monte Carlo runs were performed to evaluate the performance of unmixing algorithms under test.

Zero mean Gaussian random noise is added to the synthetic images to simulate the possible noise caused by some physical factors, such as sensor noise, *etc*. Defining *SNR* as $SNR = 10\log_{10}(E[x^T x]/E[n^T n])$, and the noise variance σ^2 can be easily determined by a particular value of *SNR*, i.e. $\sigma^2 = E[x^T x]/(10^{SNR/10} l)$. Here, where x is the pixel vector, n is the noise vector, and l is the dimensional number of both x and n.

Here, the network size of SOM is chosen as 6×6, and the fuzzy weighted index m is determined according to the inflexion of the fuzzy objective function described as Section 3.2.

5.1.2.1. Unmixing results for simulated data with linear spectral mixing. For linear spectral mixing, the synthetic images are created by directly multiplying the endmember spectral signature matrix with the standard abundance images. The unmixing results of the synthetic images with the distinct endmember set and the similar endmember set are shown in Fig. 9, respectively.

As Fig. 9 shows, in general, for simulated data with linear spectral mixing, the proposed SOM&FM has good unmixing result and stronger anti-noise ability in both cases of distinct and similar endmember sets. In detail, for distinct endmember set, FCLS and GDME get excellent unmixing results which are better than the results of SOM&FM. That is because FCLS and GDME are based on linear mixture model which accords with the simulated data source, which is generated by linear mixture. But for similar endmember set and under strong noise, they perform worse than both FCM and SOM&FM.

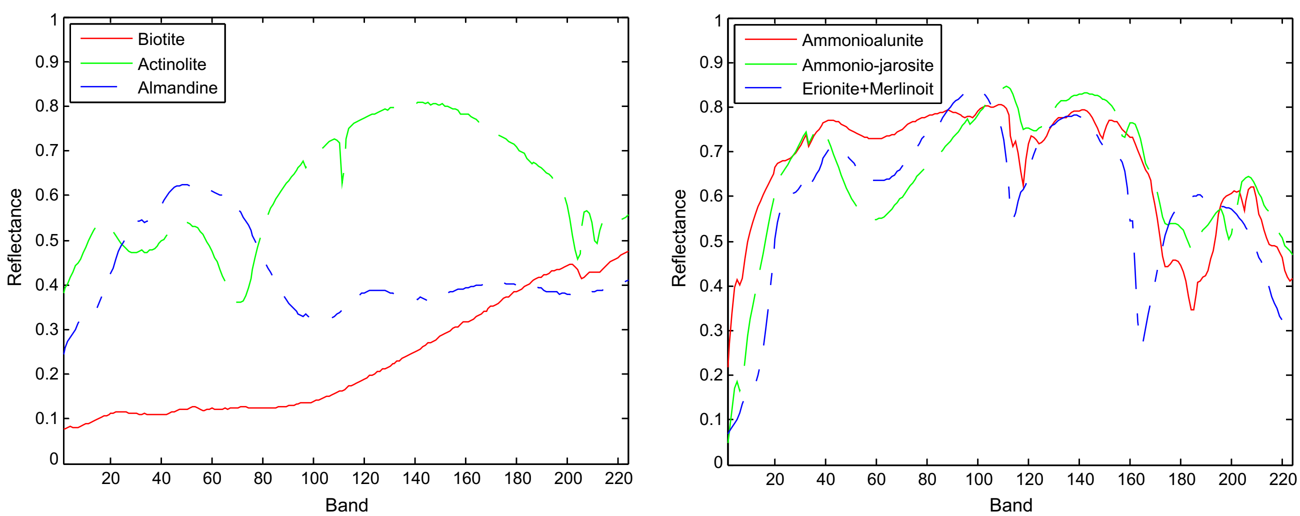

Fig. 8. The distinct endmember set (left) and the similar endmember set (right).

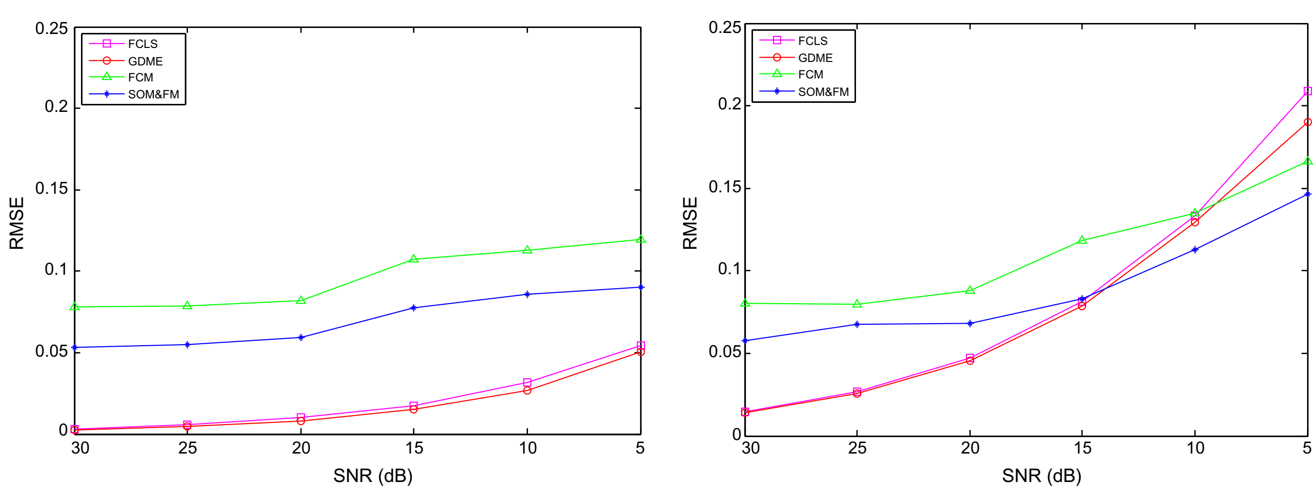

Fig. 9. The unmixing results of synthetic images in case of linear spectral mixing with the distinct endmember set (left) and the similar endmember set (right).

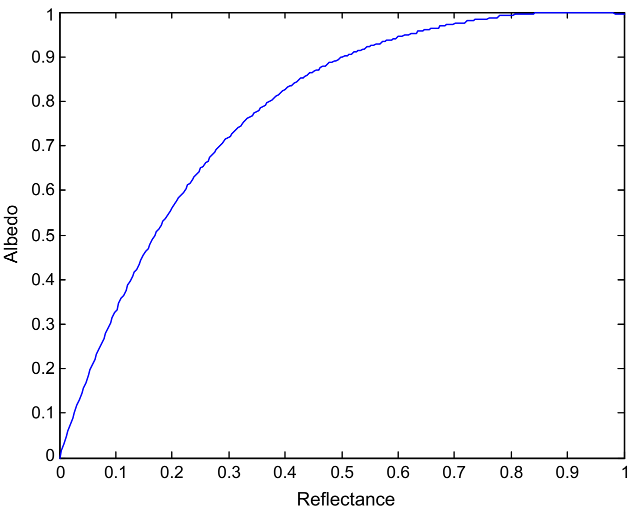

Fig. 10. The relationship between reflectance and albedo.

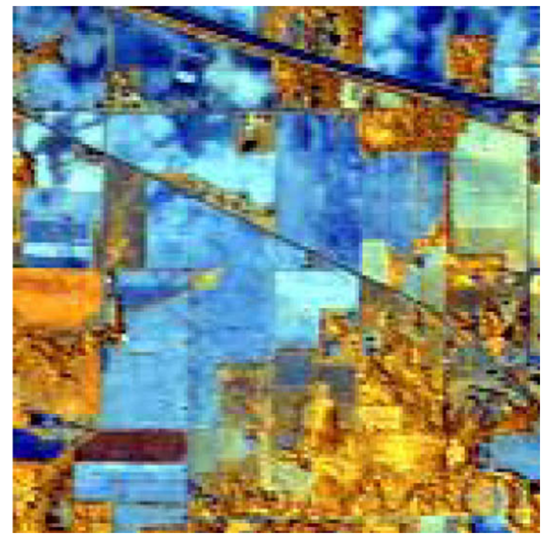

Fig. 12. Pseudo-color image of the AVIRIS.

5.1.2.2. Unmixing results for simulated data with nonlinear spectral mixing. The albedo of an intimate mixture is a linear combination of the spectral reflectances (single-scattering albedos) of its endmembers weighted by the abundance fractions. Therefore, to generate the nonlinear mixing synthetic images, endmember spectral reflectances are firstly converted to the albedos using the modified Hapke model (Jia and Qian, 2007). Secondly, unmixing linear mixing method is applied to create linear mixture of albedos. Then the resulting mixing albedos are reverted back to reflectances to generate the nonlinear mixing spectral reflectances. The relationship between reflectance $r(\lambda)$ and albedo $w(\lambda)$ is defined as

$$r(\lambda) = \frac{w(\lambda)\cos(\theta_i)[P(g)(1+B(g)) - 1 + H(\theta_i)H(\theta_c)]}{4(\cos(\theta_i) + \cos(\theta_c))}, \tag{6}$$

where r is the spectral reflectance, w is the single-scattering albedo, λ is the wavelength, θ_i and θ_c are the angles of incidence and emittance. P and B are the single-scattering phase function and the backscatter function with the phase angle g. H is the Hapke's approximation to Chandrasekhar's function, and is defined as

$$H(\theta) = \frac{1 + 2\cos(\theta)}{1 + 2\cos(\theta)(1-w)^{1/2}}. \tag{7}$$

In experiments, approximation with $B(g) = 0$ (i.e., negligible for phase angles of greater than 15°) and $P(g) = 1$. θ_i and θ_c are set to 30° and 0°, respectively. Then, the nonlinear relationship between $r(\lambda)$ and $w(\lambda)$ can be described as Fig. 10.

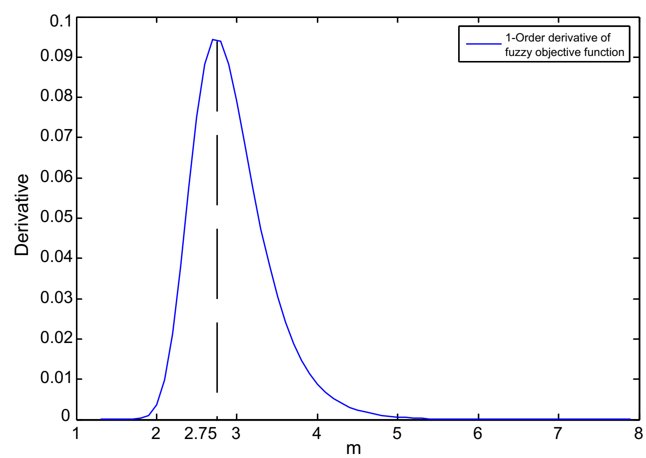

Fig. 13. The choice of m in the experiment of Indian Pine Test Site (145 × 145) AVIRIS Indian Pine Test Site Data.

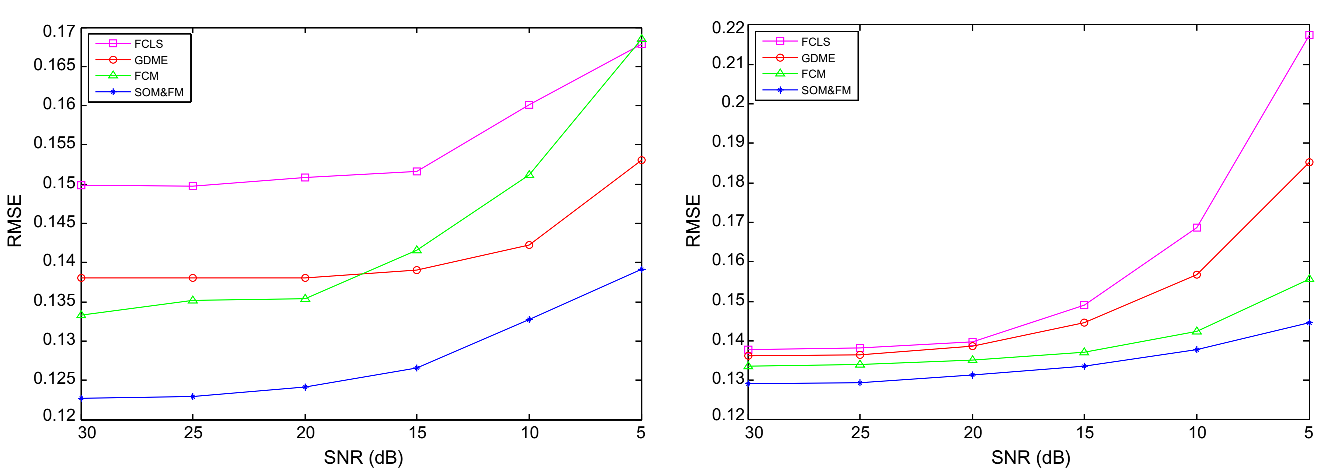

Fig. 11. The unmixing results of synthetic images in case of nonlinear spectral mixing with the distinct endmember set (left) and the similar endmember set (right).

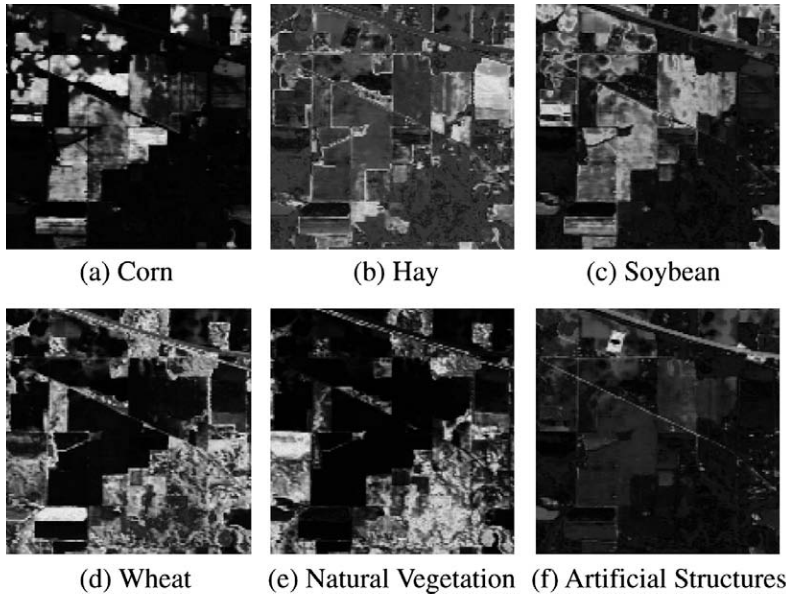

Fig. 14. Unmixing results of the AVIRIS Indian Pine Test Site hyperspectral images.

As Fig. 11 shows, for simulated data with nonlinear spectral mixing, the proposed SOM&FM method is more accurate than FCLS, GDME and FCM in different noise level with both distinct and similar endmember sets. That is because with combination of fuzzy model and neural network, the proposed SOM&FM method has stronger ability in characterizing the nonlinear relationship between individual endmembers than FCM and the LSMM-based algorithms including FCLS and GDME.

5.2. Experiment for real-world images

Because of the lack of standard abundances for real-world hyperspectral images, the unmixing method cannot be evaluated by digital indexes. However, we can evaluate the unmixing method by comparing the unmixing result with the investigated ground truth.

The real-world hyperspectral images used in this experiment is a well-known AVIRIS image scene for agriculture/forestry landscape in the Indian Pine Test Site obtained in June 1992. It is available on line (http://cobweb.ecn.purdue.edu/~biehl/MultiSpec/) and is often used for testing the performance of unmixing algorithm. It was collected by 220 spectral bands with a spectral resolution of 10 nm and a spatial resolution of 17 m. Fig. 12 shows a pseudo-color image of this region with R, G, and B being displayed with band 70, band 86, and band 136, respectively. Its image size is 145×145 pixels. As the ground truth in (Landgrebe, 1998) shows, there are some agricultures (corn, hay, soybean, and wheat), natural vegetation, and some artificial structures (tower, railways, high ways, roads and houses) in this area, and Fig. 12 also shows their distributions in some extent. The bands 104–109 and 150–163 have been removed prior to the analysis due to water absorption and low SNR in those bands. As a result, a total of 200 bands were used for the experiments.

In the experiments, we choose about 150 data samples as the training samples for training an 8×8 SOM neural network. The fuzzy weighted index m is determined according to the inflexion of the fuzzy objective function, shown as Fig. 13.

In Fig. 14a–f are the unmixing abundance matrixes of corn, hay, soybean, wheat, natural vegetation and artificial structures, respectively. By comparison, we can see that the unmixing result is very identical with the investigated ground truth (Landgrebe, 1998).

6. Conclusion

A method which combines the SOM neural network and the fuzzy membership is designed for decomposing the mixed pixels in the hyperspectral images. It firstly trains the SOM in a supervised way, and then gets the unmixing abundances by calculating fuzzy memberships. Compared with the existing methods, it relaxes the demand of prior knowledge, gets rid of the problem of the local optimum, and satisfies both the ANC and the ASC conditions. In the experimental part, we evaluated the algorithm accuracy and robusticity by synthetic data experiments, and compared it with some existing methods to demonstrate its advantages. In addition, we also showed the experimental results on real-world data. As the experimental results showed, the proposed method is suitable for decomposition of mixed pixels in hyperspectral remote sensing image, *especially* for nonlinear spectral mixing.

Acknowledgments

The authors would like to thank Prof. Chein-I Chang for offering the FCLS code and Prof. Hairong Qi for offering the GDME code. This work was supported in part by the National High Technology Research and Development Program of China (863 Program) under Grant 2009AA12Z115, the National Natural Science Foundation of China under Grant 60672116, and the Shanghai Leading Academic Discipline Project (No. B112).

References

Chang, C.-I., 2007. Hyperspectral Data Exploitation. John Wiley & Sons, Inc..
Foody, G.M., 2000. Estimation of sub-pixel land cover composition in the presence of untrained classes. Comput. Geosci. 26 (4), 469–478.
Friedman, M., Kande, A., 1999. Introduction to Pattern Recognition – Statistical, Structural, Neural, and Fuzzy Logic Approaches. World Scientific, Singapore. pp. 167–217.
Gao, X., Pei, J., Xie, W., 2000. A study of weighting exponent m in a fuzzy C-means algorithm. Acta Electron. Sin. 28 (4), 80–83.
Heinz, D.C., Chang, C.-I., 2001. Fully constrained least squares linear spectral mixture analysis method for material quantification in hyperspectral imagery. IEEE Trans. Geosci. Remote Sens. 39 (3), 529–545.
Jia, S., Qian, Y., 2007. Spectral and spatial complexity-based hyperspectral unmixing. IEEE Trans. Geosci. Remote Sens. 45 (12), 3867–3879.
Kohonen, T., 2001. Self-organizing Maps, Series in Information Sciences. Springer, Berlin, Germany.

Landgrebe, D., 1998. Multispectral Data Analysis: A Signal Theory Perspective. School of Electrical & Computer Engineering, Purdue University, West Lafayette, Indiana.
Miao, L., Qi, H., 2007. Endmember extraction from highly mixed data using minimum volume constrained nonnegative matrix factorization. IEEE Trans. Geosci. Remote Sens. 45 (3), 765–777.
Miao, L., Qi, H., Szu, H., 2007. A maximum entropy approach to unsupervised mixed-pixel decomposition. IEEE Trans. Image Process. 16 (4), 1008–1021.
Mohamed, S.N., Mohamed, A.L., Mohamed, R.B., 2004. IEEE the contribution of the sources separation method in the decomposition of mixed pixels. Trans. Geosci. Remote Sens. 42 (11), 2642–2653.
Paura, V.P., Piper, J., Plemmons, R.J., 2006. Nonnegative matrix factorization for spectral data analysis. Lin. Alg. Appl. 416 (1), 29–47.
Small, C., 2001. Estimation of urban vegetation abundance by spectral mixture analysis. Int. J. Remote Sens. 22 (7), 1305–1334.
Wang, J., Chang, C.-I., 2006. Applications of independent component analysis in endmember extraction and abundance quantification for hyperspectral imagery. IEEE Trans. Geosci. Remote Sens. 44 (9), 2601–2616.
Yu, J., Cheng, Q., Huang, H., 2004. IEEE analysis of the weighting exponent in the FCM. Trans. Systems Man Cybernet. 34 (1), 634–639.